A Broadband Coaxial Line-to-SIW Transition Using Aperture-Coupling Method

Anil Kumar Nayak, *Graduate Student Member, IEEE*, Igor M. Filanovsky, *Life Senior Member, IEEE*, Kambiz Moez, *Senior Member, IEEE*, and Amalendu Patnaik, *Senior Member, IEEE*

***Abstract*— The letter demonstrates a coaxial transmission line-to-substrate integrated waveguide (CT-SIW) transition using aperture-coupling approach. The method broadens the bandwidth (BW) and reduces the transition insertion loss (IL). Two coaxial line supports with apertures for coupling are attached at the ends of substrate integrated waveguide (SIW). The copper inlaid of the apertures increases coupling of the coaxial line to SIW and can be controlled by the aperture length and the length of the line wire put in the aperture. The transition was designed, fabricated, and experimentally evaluated. The transition provides the measured 10 dB return loss (RL) fractional BW (FBW) of 104.3%, and 15 dB RL (FBW) of 78.06%. The IL of 0.37 to 0.87 dB at 19.63–62.7 GHz frequency range was obtained. The measured results are well correlated with the simulated ones.**

***Index Terms*— Aperture-coupling, broadband enhancing, coaxial line, coaxial transmission line-to-substrate integrated waveguide (CT-SIW) transition, low insertion loss (IL), substrate integrated waveguide (SIW).**

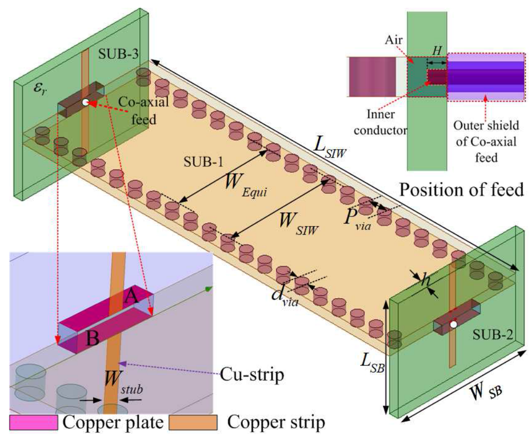

Fig. 1. Three-dimensional configuration and position of coaxial line in the transition.

I. Introduction

At the mm-wave frequency range the role of the transmission lines connecting different devices, and the transitions between different types of transmission lines becomes more critical. Any transition degrades their impedance bandwidth (BW) and adds insertion losses (ILs) [1]. Several methods were proposed to compensate these deficiencies. They include using ridge gap [2], coupled striped lines [3], ridge waveguide methods [4]–[6], and others.

The aperture-coupling feeding is proposed as an effective solution to enhance the BW and achieve better isolation amongst components such as antenna, filter, power divider, etc., [7]. This problem was addressed in [3] where the fabrication used multilayer printed circuit board (PCB) structure allowed to achieve a reliable structure. In the meantime, the substrate integrated waveguide (SIW) technique in mm-wave was also improved making high-Q 2-D components available [8]–[11], and several recent developments have described broadband transitions between the SIW and other transmission lines and waveguides [12]–[21]. In [12], a transition with close match between coaxial line and SIW has been reported using thick as well as thin substrates. This design reported 15 dB return loss (RL) with 30% fractional BW (FBW), IL less than 1.2 dB at X-band (8–12 GHz). In [13], a broadband coaxial to SIW transition with compact size, wider BW, and lower value of total loss has been reported. The losses of below 15%, 15 dB RL FBW of 48.5%, 20 dB RL FBW of 20%, and IL below 0.75 dB have been achieved. A transition between the conductor-backed-coplanar waveguide (CB-CPW) and coupled strip-line is illustrated in [14]. It investigated the linear tapered feed to improve the impedance absolute BW (ABW) to 19.95 GHz and achieved IL below 2.3 dB. Two apertures and short-circuiting patch create coupling of air-filled rectangular waveguide (RWG) to SIW for V-band [15]. A wider FBW of 35% at the center of the frequency band is obtained. In [16], a broadband transition between grounded coplanar waveguide (CPW) and substrate integrated coaxial line (SICL) has been demonstrated. It is done by connecting two copper layers through the blind vias at two sides of the ground plane. The impedance BW of 42 GHz and IL of 0.76 dB have been received. In the recent studies, novel techniques like microstrip-vertical SIW [17], wideband excitation between SIW and microstrip line [22], SIW-waveguide [18],

Manuscript received April 25, 2022; revised June 1, 2022; accepted June 7, 2022. This work was supported the Science and Engineering Research Board, Government of India, in the form of Overseas Visiting Doctoral Fellowship under Award SB/S9/Z16/2016-V(2019-20). *(Corresponding author: Kambiz Moez.)*

Anil Kumar Nayak and Amalendu Patnaik are with the Department of Electronics and Communication Engineering, IIT Roorkee, Roorkee, Uttarakhand 247667, India, and also with the Department of Electrical and Computer Engineering, University of Alberta, Edmonton, AB T6G 2R3, Canada (e-mail: anayak@ieee.org; apatnail@ieee.org).

Igor M. Filanovsky and Kambiz Moez are with the Department of Electrical and Computer Engineering, University of Alberta, Edmonton, AB T6G 2R3, Canada (e-mail: ifilanov@ualberta.ca; kambiz@ualberta.ca).

Color versions of one or more figures in this letter are available at https://doi.org/10.1109/LMWC.2022.3182933.

Digital Object Identifier 10.1109/LMWC.2022.3182933

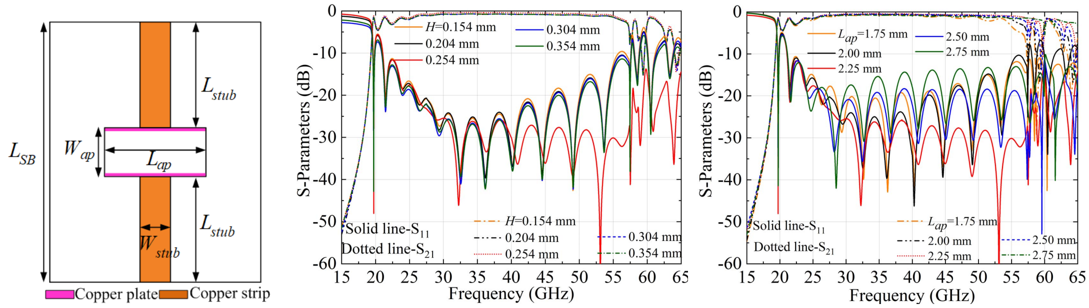

Fig. 2. (a) Coaxial line supporter with aperture (with copper inlaid) and additional copper strips (L_{SB} = 5.8, L_{ap} = 2.25, L_{stub} = 2.4, W_{stub} = 0.4, W_{ap} = 1.52, L_{SIW} = 21.7, and W_{SIW} = 6; unit: mm), $|S|$-parameters of the transition for various: (b) L_{ap} at H = 0.254 mm and (c) H at L_{ap} = 2.25 mm.

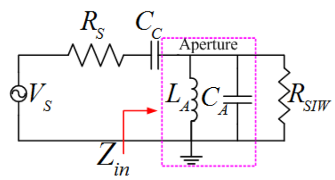

Fig. 3. Transition lumped-parameter circuit equivalent.

SIW-air-field RWG [19], microstrip-ridged empty SIW (RESIW) [20], and coaxial to SIW transition in multilayer [21] transitions have been reported.

In this letter, the aperture-coupling transition between coaxial line to SIW (CT-SIW) is designed and tested. The authors stress that the aperture-coupling approach enhances the BW with acceptable other characteristics. Design guidelines are also described. The transition is operable in the mm-wave frequency range of 19.63–62.7 GHz. The present work shows measured minimum and maximum values of RL of 10 and 65 dB, IL of 0.37 and 0.83 dB, and total loss of 20% and 40% in the entire band (except for frequencies higher than 62.7 GHz), respectively. Finally, a comparison with the previously reported results is given.

II. Transition Construction and Design

Fig. 1 shows the proposed transition. The main parts of it, denoted as SUB-1, SUB-2, and SUB-3 are using PCB with the board thickness h = 0.508 mm. Part SUB-1 is used for SIW realization.

The design procedure is described by the following sequence of steps.

1) The design frequency of the SIW was decided as 19–65 GHz. The length L_{SIW} and width W_{SIW} of the SIW (see Fig. 1) were chosen for 19–65 GHz band following the SIW design guidelines reported in [8]–[11], [23]–[25]. The SIW cut-off frequency is 18.94 GHz.
2) The diameter $d_{via} \leq (\lambda/5)$, where λ is the guided wavelength at 40 GHz (center frequency of the range), pitch distance $P_{via} \leq 2d_{via}$ of the metallic vias of the row, and equivalent width of SIW W_{Equi} ($W_{Equi} = W_{SIW} - 1.08(d_{via}^2/P_{via}) + 0.1(d_{via}^2/W_{SIW})$) were decided by the cutoff frequency at TE_{10}. The sizes are d_{via} = 0.6 mm and P_{via} = 1.1 mm.
3) The dimensions of support pieces L_{SB} = 5.8 mm and W_{SB} = 7.8 mm are chosen to provide a convenient mechanical connection with the coaxial line and SIW.
4) These support pieces have an aperture of size L_{ap} = 2.25 mm, W_{ap} = 1.52 mm ($\approx 3 \times h$), and on the side of SIW, have two copper strips (stubs) L_{stub} = 2.4 mm = 0.45λ and W_{stub} = 0.4 mm [see Fig. 2(a)]. Two copper plates A and B [see Fig. 1, left corner, and Fig. 2(a)] are positioned at the inner walls of the slot. The plates, together with stubs, are connected to the coaxial line grounded outer shell.
5) The length H of naked wire inside the aperture (see Fig. 1, right corner) was chosen for optimal performance after parametric analysis by simulations.

The aperture slot can be represented [3] as a parallel LC-circuit, L_A, C_A in our case. Using this idea one can represent the whole transition by the lumped parameter equivalent (see Fig. 3). For this equivalent $Z_{in}(s) = (R_{SIW}[1 + L_A(C_A + C_C)s^2] + L_As)/(C_Cs[R_{SIW}(1 + L_AC_As^2) + L_As])$. Considering now $\Gamma_{in}(s = j\omega) = (Z_{in} - R_s)/(Z_{in} + R_s) = S_{11}$. Modifying the elements of this circuit so that $L_A \to \infty$, $C_A \to 0$, and $C_C \to \infty$ brings the circuit to the condition of ideal matching (when, of course, $R_s = R_{SIW}$). Hence, increasing L_A (including the length of plates and adding the stubs), increasing the distance between the plates, and finding the maximum value of C_C (by simulations) were our guidelines to improve the transition characteristics.

The aperture slot is the place where electromagnetic (EM)-wave changes from TEM-mode to TE_{10}-mode. It is desirable that the aperture slot operates as an intermediate half-wavelength ($\lambda/2$) resonator between the line and SIW. This provides a stronger coupling and improves the impedance BW.

The length H, as was mentioned above, is set by simulations [see Fig. 2(b)]. H is varied uniformly from 0.154 to 0.354 mm with a step size of 0.05 mm. Variation in H is influencing both RL and IL. As a result, the value of H is fixed at 0.254 mm or 0.0474 λ (in practice 0.25 mm). The length of the aperture L_{ap} is also set by parametric analysis [see Fig. 2(c)]. L_{ap} is varied from 1.75 to 2.75 mm with a step size of 0.25 mm. It can be noted that RL decreases with increasing L_{ap} and vice versa. At the same time, the IL is also changing with the variation in L_{ap}. The RL and IL are found best at the specific L_{ap}, fixed at 2.25 mm. The structure was simulated using HFSS ver.2020R2 with the RT/duroid 5880LZ substrate having ε_r = 1.96 (±0.04), h = 0.508 mm, and $\tan\delta$ = 0.0019 in the proposed design. The electric and magnetic field patterns are shown in Fig. 4(a) and (b),

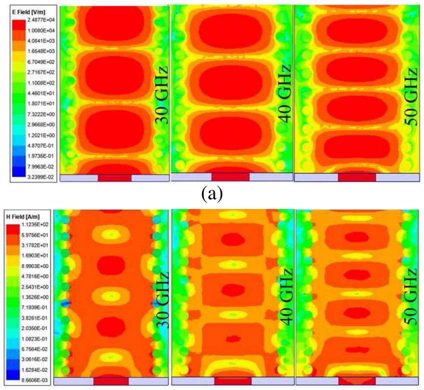

Fig. 4. Field distribution at 30, 40, and 50 GHz (from left to right): (a) electric field and (b) magnetic field.

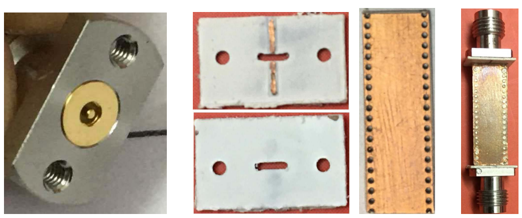

(a) (b) (c) (d)

Fig. 5. Fabricated back-to-back prototype: (a) co-axial connector (model no: 26-HV-RSR2-ND), (b) internal and external view of coaxial line support, (c) SIW part of the transition, and (d) 3-D view of transition with connectors.

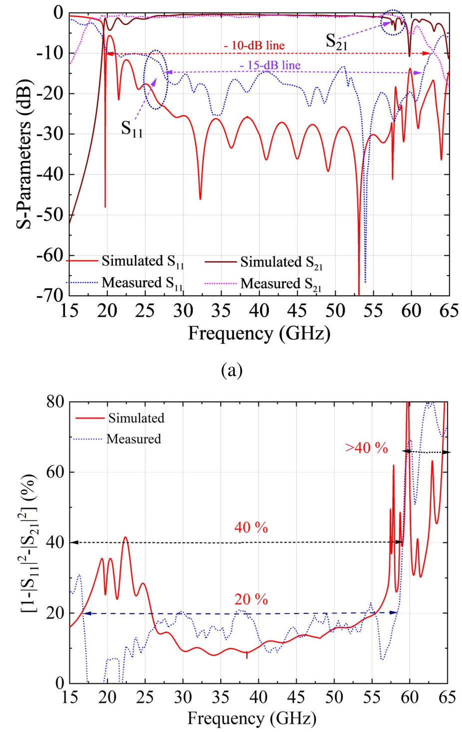

Fig. 6. Characteristics of the transition: (a) S_{11} and S_{21}, and (b) total loss.

respectively, and Fig. 4(a) confirms that only the fundamental mode (TE_{10}) exists, and the higher mode (TE_{20}) is suppressed in the SIW with the proposed method of excitation.

III. Results, Discussion, and Comparison

The satisfactory simulation results allowed us to fabricate the proposed structure; a laboratory prototype is developed. The parts of the back-to-back CT-SIW transition and its connector are demonstrated in Fig. 5(a)–(d). Three parts (SUB-1–SUB-3) are glued together with the Feviquick solution [26], [27]. The experiments are carried out using co-axial connectors (model no: 26-HV-RSR2-ND) with frequency up to 67 GHz and Agilent N5247A (10 MHz–67 GHz) vector network analyzer (VNA). Moreover, the electronics calibration (Ecal) method has been used to do the experimental validation. The measurements were taken up to the frequency of 65 GHz. The simulated and experimental *S*-parameters (S_{11} and S_{21}) of the proposed CT-SIW transition are presented in Fig. 6(a). From this plot, the measured RL is better than 10 dB from 19.63 to 62.7 GHz and is above 15 dB from 27 to 61.57 GHz. At the same time, the simulated RL is above 10 dB from 20.25 to 65 GHz and is better than 15 dB from 22.64 to 65 GHz. The experimental IL is below 0.37 dB (minimum) and 0.83 dB (maximum) in the whole band except for the narrow region from 60 to 65 GHz. In contrast, the minimum and maximum simulated ILs are 0.37 and 0.83 dB in the whole band, except the frequency ranges from 20 to 22.83 GHz (lower end) and from 60 to 65 GHz (higher end). It means that measured minimum and maximum ILs are about 0.013 and 0.029 dB/mm in the whole band (except of 60–65 GHz), respectively. Moreover, an early change in the transition phase (not shown) marks the low loss in the structure at the specified frequency band in the design.

TABLE I
Comparison of Competitive Broadband Transition

Ref.	Freq.(GHz)	Structure	RL (dB)	IL (dB)	BW (GHz/%)
[13]	8-12	CT-SIW	$\geq$ 15	$\leq$ 0.75	4/48.5
[15]	50-75	RWG-SIW	$\geq$ 10	$\leq$ 0.58	25/35
[16]	0-42	SICL-CPW	$\geq$ 10	$\leq$ 0.76	42/NR
[17]	33-36.7	MS-SIW	$\geq$ 15	$\leq$ 0.95	3.7/10.57
[12]	8-12	CT-SIW	$\geq$ 15	$\leq$ 1.2	4/30
[3]	48.6-67	MS-SIW	$\geq$ 10	$\leq$ 2.5	18.4/42.3
This work	**19.63-62.7 27-61.57**	**CT-SIW**	**$\geq$ 10 $\geq$ 15**	**$\leq$ 0.83 $\leq$ 0.37**	**43.07/104.53 34.57/78.06**

The simulated and measured total losses are plotted in Fig. 6(b). The loss is low (<20% and <40%) at the specified frequency range. However, the loss is higher (>40%) in the range of 60–65 GHz. Table I illustrates the performance of the proposed transition and compares it with the previously known results. The proposed design operates at the mm-wave frequency (19–65 GHz) and has the benefits of easy fabrication, large BW, low IL, and total loss below 20%.

IV. Conclusion

In this letter, an aperture-coupled-based broadband CT-SIW transition is presented. It is implemented using PCB technology. The simulation proves that the proposed transition offers competitive advantages such as wider impedance BW, low IL, and low total loss (<20%). Finally, the prototype back-to-back CT-SIW is fabricated and measured to validate the transition operation and performance.

References

[1] J. Navarro, K. Chang, J. Tolleson, S. Sanzgiri, and R. Lee, "A 29.3-GHz cavity-enclosed aperture-coupled circular-patch antenna for microwave circuit integration," *IEEE Microw. Guided Wave Lett.*, vol. 1, no. 7, pp. 170–171, Jul. 1991.

[2] M. Fakharzadeh and S. Jafarlou, "A broadband low-loss 60 GHz die to rectangular waveguide transition," *IEEE Microw. Wireless Compon. Lett.*, vol. 25, no. 6, pp. 370–372, Jun. 2015.

[3] T. Zhang, L. Li, Z. Zhu, and T. J. Cui, "A broadband planar balun using aperture-coupled microstrip-to-SIW transition," *IEEE Microw. Wireless Compon. Lett.*, vol. 29, no. 8, pp. 532–534, Aug. 2019.

[4] A. R. Mallahzadeh and S. Esfandiarpour, "Wideband H-plane horn antenna based on ridge substrate integrated waveguide (RSIW)," *IEEE Antennas Wireless Propag. Lett.*, vol. 11, pp. 85–88, 2012.

[5] Y. Zhao, Z. Shen, and W. Wu, "Wideband and low-profile H-plane ridged SIW horn antenna mounted on a large conducting plane," *IEEE Trans. Antennas Propag.*, vol. 62, no. 11, pp. 5895–5900, Nov. 2014.

[6] S. Choudhury, A. Mohan, P. K. Mishra, and D. Guha, "Wideband pyramidal ridged horn design by SIW technology," *IEEE Antennas Wireless Propag. Lett.*, vol. 18, no. 7, pp. 1517–1521, Jul. 2019.

[7] R. Q. Lee and R. N. Simons, "Coplanar-waveguide aperture-coupled microstrip patch antenna," *IEEE Microw. Guided Wave Lett.*, vol. 2, no. 4, pp. 138–139, Apr. 1992.

[8] D. Deslandes and K. Wu, "Accurate modeling, wave mechanisms, and design considerations of a substrate integrated waveguide," *IEEE Trans. Microw. Theory Techn.*, vol. 54, no. 6, pp. 2516–2526, Jun. 2006.

[9] M. Bozzi, A. Georgiadis, and K. Wu, "Review of substrate-integrated waveguide circuits and antennas," *IET Microw., Antennas Propag.*, vol. 5, no. 8, pp. 909–920, Jun. 2011.

[10] D. Deslandes, "Design equations for tapered microstrip-to-substrate integrated waveguide transitions," in *IEEE MTT-S Int. Microw. Symp. Dig.*, May 2010, pp. 704–707.

[11] Z. Kordiboroujeni and J. Bornemann, "New wideband transition from microstrip line to substrate integrated waveguide," *IEEE Trans. Microw. Theory Techn.*, vol. 62, no. 12, pp. 2983–2989, Dec. 2014.

[12] S. Mukherjee, P. Chongder, K. V. Srivastava, and A. Biswas, "Design of a broadband coaxial to substrate integrated waveguide (SIW) transition," in *Proc. Asia–Pacific Microw. Conf. Proc. (APMC)*, Nov. 2013, pp. 896–898.

[13] A. A. Khan and M. K. Mandal, "A compact broadband direct coaxial line to SIW transition," *IEEE Microw. Wireless Compon. Lett.*, vol. 26, no. 11, pp. 894–896, Nov. 2016.

[14] W.-J. Lu, Y.-M. Bo, and H.-B. Zhu, "A broadband transition design for a conductor-backed coplanar waveguide and a broadside coupled stripline," *IEEE Microw. Wireless Compon. Lett.*, vol. 22, no. 1, pp. 10–12, Jan. 2012.

[15] Y. Li and K.-M. Luk, "A broadband V-band rectangular waveguide to substrate integrated waveguide transition," *IEEE Microw. Wireless Compon. Lett.*, vol. 24, no. 9, pp. 590–592, Sep. 2014.

[16] S. Yang, Z. Yu, and J. Zhou, "A low-loss broadband planar transition from ground coplanar waveguide to substrate-integrated coaxial line," *IEEE Microw. Wireless Compon. Lett.*, vol. 31, no. 11, pp. 1191–1194, Nov. 2021.

[17] X. Dai, "An integrated millimeter-wave broadband microstrip-to-waveguide vertical transition suitable for multilayer planar circuits," *IEEE Microw. Wireless Compon. Lett.*, vol. 26, no. 11, pp. 897–899, Nov. 2016.

[18] J. Dong, Y. Liu, Z. Yang, H. Peng, and T. Yang, "Broadband millimeter-wave power combiner using compact SIW to waveguide transition," *IEEE Microw. Wireless Compon. Lett.*, vol. 25, no. 9, pp. 567–569, Sep. 2015.

[19] I. Mohamed and A. Sebak, "Broadband transition of substrate-integrated waveguide-to-air-filled rectangular waveguide," *IEEE Microw. Wireless Compon. Lett.*, vol. 28, no. 11, pp. 966–968, Nov. 2018.

[20] D. Herraiz, H. Esteban, J. A. Martínez, A. Belenguer, and V. Boria, "Microstrip to ridge empty substrate-integrated waveguide transition for broadband microwave applications," *IEEE Microw. Wireless Compon. Lett.*, vol. 30, no. 3, pp. 257–260, Mar. 2020.

[21] S. Ebadi, N. Landy, M. Perque, T. Driscoll, and D. Smith, "Wideband coaxial to substrate-integrated waveguide transition in a multilayer reconfigurable antenna configuration," in *Proc. IEEE Antennas Propag. Soc. Int. Symp. (APSURSI)*, Jul. 2014, pp. 454–455.

[22] P. Wu, J. Liu, and Q. Xue, "Wideband excitation technology of TE_{20} mode substrate integrated waveguide (SIW) and its applications," *IEEE Trans. Microw. Theory Techn.*, vol. 63, no. 6, pp. 1863–1874, Jun. 2015.

[23] M. Pasian, M. Bozzi, and L. Perregrini, "A formula for radiation loss in substrate integrated waveguide," *IEEE Trans. Microw. Theory Techn.*, vol. 62, no. 10, pp. 2205–2213, Oct. 2014.

[24] F. Xu and K. Wu, "Guided-wave and leakage characteristics of substrate integrated waveguide," *IEEE Trans. Microw. Theory Techn.*, vol. 53, no. 1, pp. 66–73, Jan. 2005.

[25] A. K. Nayak, I. M. Filanovsky, K. Moez, and A. Patnaik, "Broadband conductor backed-CPW with substrate-integrated coaxial line to SIW transition for C-band," *IEEE Trans. Circuits Syst. II, Exp. Briefs*, vol. 69, no. 5, pp. 2488–2492, May 2022.

[26] A. Sharma, G. Das, P. Ranjan, N. K. Sahu, and R. K. Gangwar, "Novel feeding mechanism to stimulate triple radiating modes in cylindrical dielectric resonator antenna," *IEEE Access*, vol. 4, pp. 9987–9992, 2016.

[27] R. K. Gangwar, P. Ranjan, and A. Aigal, "Wideband four-element two-segment triangular dielectric resonator antenna with monopole-like radiation," *Int. J. Microw. Wireless Technol.*, vol. 9, no. 2, pp. 411–418, Mar. 2017.